

## Mitigating plastic pollution at sea: Natural seawater degradation of a sustainable PBS/PBAT marine rope

Le Gué Louis <sup>1,2,\*</sup>, Davies Peter <sup>1</sup>, Arhant Mael <sup>1</sup>, Vincent Benoit <sup>2</sup>, Tanguy Erwan <sup>3</sup>

<sup>1</sup> Ifremer RDT, Research and Technology Development Unit, 1625 route de Sainte-Anne, Plouzané, 29280, France

<sup>2</sup> DECOD (Ecosystem Dynamics and Sustainability), IFREMER, INRAE, Institut Agro, Lorient, 56325, France

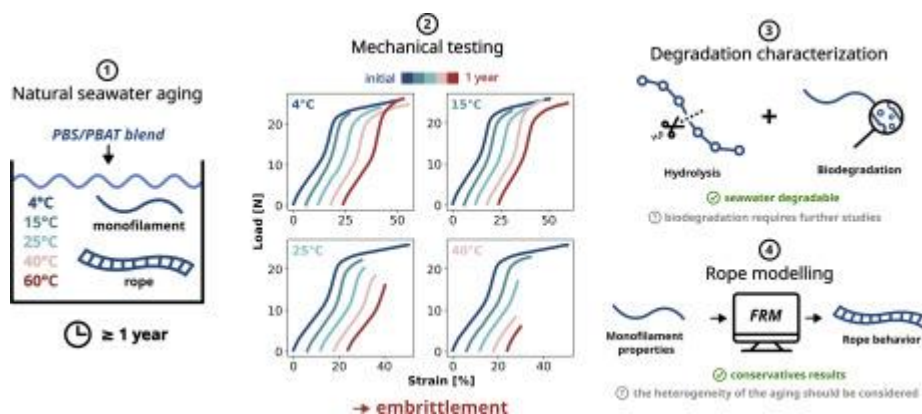
<sup>3</sup> Le Drezen, 12 rue de Kélaireun, Le Guilvinec, 29730, France

\* Corresponding author : Louis Le Gué, email address : [louis.le.gue@ifremer.fr](mailto:louis.le.gue@ifremer.fr)

### Abstract :

This paper evaluates the use of a PBS/PBAT biodegradable rope to reduce the environmental impact of fishing gear lost at sea. The study aims to better understand the degradation mechanisms that the rope and its monofilaments may encounter due to the long term exposure to seawater. The monofilaments were immersed in natural seawater for up to 18 months, and rope samples were also immersed to study aging at a larger scale and evaluate the ability of a modelling tool to predict initial and aged states of the rope. At low temperatures, no loss of properties was observed for the monofilament and rope. However, at higher temperatures, biodegradation and hydrolysis processes were observed, leading to a faster loss of properties in the monofilament compared to the rope. The modelling tool provided conservative predictions due to severe mechanical test conditions of aged monofilament and a degradation gradient within the rope structure.

### Graphical abstract



---

## Highlights

► A rope made of braided PBS/PBAT monofilaments has been tested and aged. ► A PBS/PBAT rope could last at least 1 year and a half in seawater at 4 °C and 15 °C. ► Biodegradation and hydrolysis were observed for PBS/PBAT monofilaments at 25 °C. ► A numerical tool has been used to predict initial and aged properties of the rope.

**Keywords** : Plastic pollution, Biopolymer, Seawater aging, Polybutylene succinate, Rope structure, Numerical simulation

---

30 **1. Introduction**

31 Since awareness of plastic pollution in the oceans has increased, initiatives to reduce the use of single-  
32 use plastics, which are the most common type of waste found on the coast (Morales-Caselles et al., 2021),  
33 have been launched. However, even if no plastic entered via the coast or rivers, the problem of plastic  
34 pollution in our oceans would not be solved: more than 30% of the plastic waste in the open sea consists  
35 of synthetic ropes coming from ocean pathways (Morales-Caselles et al., 2021). Furthermore ropes used for  
36 fishing applications are the major source of entanglement for marine species (Johnson et al., 2005; Galgani  
37 et al., 2018), for example 83% of the population of the endangered *Eubalaena glacialis* had been entangled  
38 at least once (Knowlton et al., 2012). Entangled animals can die rapidly by drowning and sink, or be  
39 entangled for a long period and die slowly (Moore et al., 2006). Several ways to reduce the impact of ropes  
40 have been investigated in the past, such as enhancing the visibility of the gear to reduce the risk of contact

41 (Kraus et al., 2014), or limiting rope strength to increase the survival rate post-entanglement (Knowlton  
42 et al., 2016). But after a possible ghost fishing period, the gear disintegrates into particles less than 5 mm,  
43 known as microplastics (Wright et al., 2021). Microplastics thus produced will accumulate in the sediment  
44 (Van Cauwenberghe et al., 2013), be ingested by marine organisms (Wright et al., 2013), and affect a large  
45 number of species after entering the food chain by trophic transfers (Carbery et al., 2018).

46 Recently, the development of biodegradable polymer monofilaments has provided new ways to mitigate  
47 the environmental impact of derelict gear. Gear made of this kind of material could reduce the entanglement  
48 rate by limiting the accumulation of lost gear and facilitating the disentanglement process by the loss of  
49 properties. It could also tackle the microplastics pollution by being completely mineralized by the organisms  
50 present in the marine environment, and avoid the release of toxic chemicals by being additive free. However,  
51 such materials must strike a delicate balance, possessing the ability to maintain their mechanical strength  
52 for a sufficiently long period of time to be usable, while also having the capability to degrade or break  
53 down fast enough in order to minimize the impact of loss. Among biopolymers, polylactide (PLA) is  
54 the most common (European Bioplastics e.V., 2020). This bio-based polymer is processable into fibres  
55 (Puchalski et al., 2017; Le Gall et al., 2022) which could be braided into ropes (Furuike et al., 2015).  
56 However PLA does not degrade in seawater under natural conditions as shown by several authors (Deroiné,  
57 2014; Bagheri et al., 2017; Huang et al., 2020), so it is not suitable for reducing the impact of current  
58 persistent materials. Polyhydroxyalkanoates (PHA) are microbial polyesters (Saito and Doi, 1994) known  
59 to be degraded by microorganisms living in seawater (Doi et al., 1990; Savenkova et al., 2000; Wang et al.,  
60 2004; Thellen et al., 2008; Numata et al., 2009; Volova et al., 2010; Deroiné et al., 2015; Dilkes-Hoffman  
61 et al., 2019). Nevertheless PHA fibres are very difficult to process due to a narrow window of processing  
62 temperatures (Luzier, 1992), which limits their industrial applications and explains why, at the time of  
63 writing, no PHA fibres are commercially available. In addition, according to the result of Dilkes-Hoffman  
64 et al. (2019), a PHA monofilament with a thickness of 0.3 mm would last less than a year. Considering their  
65 expensive production cost (Mozejko-Ciesielska and Kiewisz, 2016), a rope or a net made of PHA would not  
66 be economically beneficial for users. In the absence of a law compelling the use of this type of material, such  
67 gear would not be used widely enough to address the problem of plastic pollution by lost gear. Chemically  
68 modified polymers with adjustable biodegradation rate are also in development (Martin et al., 2014; Samadi  
69 et al., 2019; Rheinberger et al., 2021), but are not commercially available as fibres at the time of writing.  
70 Polybutylene succinate (PBS) is a promising biopolymer which presents a low melting temperature, a good  
71 thermal stability, and suitable mechanical properties (Freyermouth, 2014). PBS is an aliphatic polyester  
72 produced through a two-step polymerization process, consisting of the esterification of succinic acid and  
73 1,4-butanediol, followed by a transesterification (Xu and Guo, 2010; Sisti et al., 2016). Succinic acid is  
74 typically petroleum-derived, however it can also be biosourced through bacterial fermentation (Song and  
75 Lee, 2006). Similarly, 1,4-butanediol is primarily petroleum-sourced for industrial applications (De Munck,

76 1980; Harris et al., 1980), yet it can also be obtained from various biomass precursors such as the catalytic  
77 reduction of biosourced succinic acid, direct synthesis from biomass, or thermolysis of a PHA derived from  
78 biomass (Sisti et al., 2016). The marine ecotoxicity of PBS and bioplastics in general is a topic that is  
79 currently not well addressed in the literature. After a 28 day and 2 year observation of PBS buried in soil,  
80 Adhikari et al. (2016) found that the diversity of biomass was not affected by the degradation of PBS, while  
81 a reduction was observed in the aging of PA6,6. Based on these findings, PBS is a healthier alternative than  
82 the synthetic plastic materials currently in use such as PA6. According to a study by Zimmermann et al.  
83 (2020), the toxicity of commercial bioplastics, including PBS, was found to be primarily influenced by the  
84 additives used rather than the monomer itself and PBS was identified as the safest synthetic polymer among  
85 the bioplastics tested in the study. PBS biodegradation in the marine environment has been described  
86 as slow by Narancic et al. (2018) and Nakayama et al. (2019). The biodegradation of aliphatic polyester  
87 monofilaments was also investigated by Sekiguchi et al. (2011), who immersed them in the deep sea for  
88 one year. The study revealed that while PBS underwent degradation, it occurred at significantly slower  
89 rates compared to poly( $\epsilon$ -caprolactone) and poly(b-hydroxybutyrate/valerate). Poly(butylene adipate-co-  
90 tephthalate) is an aliphatic-aromatic co-polyester obtained by the poly-condensation of 1,4-butanediol, adipic  
91 acid and terephthalic acid (Jian et al., 2020). The properties of PBAT make it suitable for industrial use  
92 in various domains, including packaging, hygiene products, and biomedical fields (Ferreira et al., 2019).  
93 As for 1,4-butanediol and succinic acid, terephthalic acid is mainly petroleum-based but could be bio-  
94 based (Tachibana et al., 2015). PBAT is known to be compostable and biodegradable in soil environments  
95 (Müller et al., 2001). However, similar to PBS, its degradation in the marine environment has received  
96 limited attention and few studies have been conducted on this topic, but all the authors agree on the slow  
97 rate of degradation of PBAT in the marine environment (Kedzierski et al., 2018; Nakayama et al., 2019;  
98 De Monte et al., 2022; Delacuvellerie et al., 2023). PBAT's higher ductility compared to PBS makes it an  
99 ideal plasticizer for blending, resulting in a polymer blend with tailored properties (de Matos Costa et al.,  
100 2020). PBS/PBAT and PBSAT have already been used to manufacture less impacting fishing gear such as  
101 gillnets, traps and longlines (Seonghun et al., 2014; Kim et al., 2016; Grimaldo et al., 2018a, 2019; Seonghun  
102 et al., 2020; Grimaldo et al., 2020; Cerbule et al., 2022a,b). Authors agree that the slow degradation of  
103 monofilament can reduce the ghost fishing period in the event of a loss (Grimaldo et al., 2019, 2018b; Kim  
104 et al., 2018, 2019; Seonghun et al., 2020; Brakstad et al., 2022). PBS/PBAT blends are therefore suitable  
105 for the development of a new generation of less impacting marine ropes, but the conflicting specifications  
106 require a detailed understanding of the behaviour of this type of rope when used at sea for long periods.  
107 However, testing ropes requires significant resources and materials. The present study focuses first on the  
108 natural degradation of a PBS/PBAT monofilament immersed in seawater at temperatures from 4 to 60°C.  
109 Mechanical property degradation is then investigated and damage mechanisms are clarified. Data from these  
110 tests are then used to predict the aging of a braided rope, using the properties of the monofilament at both

111 initial and aged states.

## 112 **2. Material and methods**

### 113 *2.1. Material*

114 Two types of samples were studied: a braided rope with 8 strands each composed of 8 yarns with 21  
115 monofilaments as shown in Figure 1, and the monofilament extracted from the rope. The monofilament was  
116 extruded, and the rope manufactured by Le Drezen (Le Guilvinec, France). The monofilament is colorless  
117 with a diameter of 0.35 mm, and obtained by extrusion and drawing of a PBS/PBAT blend. It has a density  
118 of 1.25 g.cm<sup>-3</sup> and a molecular weight by number of 25.6 kg.mol<sup>-1</sup> with a polydispersity of 4.8. The dry  
119 glass transition temperature of this polymer is 70°C and the melt temperature is 117°C with a melting  
120 enthalpy of 60 J.g<sup>-1</sup>.

121 For comparison purposes, a monofilament extracted from a commercial high density polyethylene (HDPE)  
122 twine was also tested. Table 1 summarizes the mean properties of both monofilaments obtained by testing  
123 20 monofilaments for each material.

### 124 *2.2. Natural seawater aging*

125 The samples were immersed in natural renewed seawater from the Brest estuary maintained at several  
126 temperatures. Monofilament samples were aged at 4°C, 15°C, 25°C, 40°C and 60°C for up to 18 months and  
127 removed regularly, every month over the first year, for characterization. Rope samples were spliced then  
128 immersed at 15°C and 40°C and removed for testing according to the results obtained on the monofilaments.

### 129 *2.3. Gel permeation chromatography (GPC)*

130 After dissolving the samples in a TCM chloroform solution for 24 hours, Steric Exclusion Chromatography  
131 (SEC) was performed at 30°C, with an injection volume of 100 μL, a flow rate of 1.0 mL.min<sup>-1</sup> an Agilent-  
132 DRI refractive index detector and three columns: a PS/DVB Agilent 5 μm precolumn, and two Agilent  
133 Mixed-C 5 μm columns. Calibration was performed with chloroform as well and polystyrene standards.

### 134 *2.4. SEM observations*

135 Surface observations on pristine and aged samples were obtained by Scanning Electron Microscopy (SEM)  
136 using FEI Quanta 200 equipment. Samples were coated with a 60% gold and 40% palladium coating before  
137 being placed in the microscope.

138 *2.5. Mechanical testing*

139 Mechanical testing of monofilament samples was carried out in tension with an Instron 10 kN capacity  
140 test machine equipped with a 50 N load cell and pneumatic yarn grips. The displacement rate was 50  
141  $mm.min^{-1}$  and the strain was obtained by using two cameras to follow two markers on the monofilament.  
142 20 tests were performed for the monofilament at the initial state, then for aged samples at least 3 samples  
143 were tested for each condition of immersion time and temperature. All the tests were conducted in a  
144 laboratory maintained at 21°C and 50% relative humidity.

145 A servo-hydraulic test machine equipped with a 300 kN AEP TC4 load cell was used to test the rope  
146 samples. For the test of the rope sample at the initial state, the strain was measured using cameras following  
147 markers shown on Figure 2. For aged samples, a 250 mm wire transducer was used to measure strain in the  
148 central section in order to determine initial stiffness. The initial and aged samples stiffness were determined  
149 by calculating the slope between 1 and 5 kN. For each condition, a 5-meter-long sample with eye splices at  
150 both ends was tested with a free length of approximately 2 meters between splices. Spliced samples were  
151 connected to the machine using shackles.

152 *2.6. Mechanical modelling*

153 The software Fibre Rope Modeller (FRM) developed by Tension Technology International (TTI) was  
154 used to model the rope. FRM allows the prediction of the mechanical properties of a rope based on the  
155 properties of the individual fibers or yarn and the rope construction (Banfield et al., 2001). This hierarchical  
156 model calculates the strain energy at each level and uses the virtual work principle to determine the rope  
157 response in tension and torsion. This software was used here to predict the properties of both the initial  
158 and aged states of the rope.

159 **3. Results**

160 *3.1. Initial characterization of the monofilament and comparison with a commercial HDPE*

161 Tensile test curves obtained for the PBS/PBAT blend and the HDPE are shown on Figure 3 and the  
162 mechanical properties determined from these curves are presented in the Table 1. With a Young's modulus  
163 of 0.79 GPa and a stress at break of 261 MPa the PBS/PBAT monofilament properties are below those of  
164 the HDPE, which exhibits a Young's modulus and a stress at break respectively of 1.90 GPa and 368 MPa.

165 *3.2. Long term property changes of a PBS/PBAT monofilament immersed in seawater*

166 *3.2.1. Mechanical property changes*

167 Every month at least three samples of the PBS based monofilament were retrieved from the seawater  
168 tanks and mechanically tested to study the changes in mechanical properties of the material for different

169 immersion times and temperatures. Three samples of the HDPE monofilament were also retrieved after 6 and  
170 12 months of immersion. Figure 4 shows the tensile mechanical response of the PBS/PBAT monofilament  
171 at different immersion times and temperatures. An origin offset on each of the curve has been applied for  
172 clarity. Figure 5 summarizes the variation of the load at break with the immersion time for both materials  
173 where the error bars represent the scatter (minimum and maximum values) and the grey area represents  
174 the initial variability observed in Figure 3. The PBS/PBAT monofilament showed no significant changes  
175 in behavior or loss of load at break after being immersed for 18 months at temperatures of 4°C and 15°C.  
176 At 25°C the PBS/PBAT monofilament gradually lost its mechanical properties as seen in Figure 4 until  
177 it reached a breaking strength 38% lower than in the initial state. At the same temperature the HDPE  
178 monofilament showed no loss after 1 year, as depicted in Figure 6, which presents the tensile curves for both  
179 monofilaments after 1 year of immersion at 25°C. After 6 months at 40°C, the samples became brittle and  
180 began to break near the tensile clamps. A loss of strength of 74% was observed after 12 months at 40°C.  
181 After 4 months at 60°C, the PBS/PBAT monofilament became so brittle that it was no longer strong enough  
182 to be handled and mounted on the test machine. From 4°C to 60°C, the HDPE monofilament showed no  
183 loss of properties and even a slight increase.

### 184 3.2.2. Surface characterization by SEM

185 Figure 7 shows the surface changes samples during immersion in natural seawater. At 4°C and 15°C,  
186 no surface modification was observed, and the surfaces appear to be as new as the initial samples. For the  
187 samples at 25°C, as early as 3 months holes started to appear on the surface, and these became larger and  
188 deeper with time, leading to the surface aspect seen on the Figure 7 (d) after 18 months of immersion. To  
189 further understand the cause of the surface degradation, PBS/PBAT samples were immersed in deionized  
190 and sterilized water for 6 months. The difference in surface morphology between 6 months in renewed  
191 natural seawater and 6 months in deionized and sterilized water is shown in Figure 8. No surface erosion  
192 was observed on the sample immersed in deionized and sterilized water, whereas the surface of the sample  
193 immersed in natural seawater was severely damaged. After 12 months at 40°C, small cracks are visible on  
194 the surface of the monofilament and a strip looks as if it has been peeled off. The sample observed after 3  
195 months of immersion at 60°C exhibited lengthwise cracks, which were evenly distributed across the surface  
196 of the monofilament. Additionally, in some areas, the surface of the filament was observed to peel off.

### 197 3.2.3. PBS/PBAT monofilament hydrolysis monitored by steric exclusion chromatography

198 The molecular weights at different immersion temperatures are presented on Figure 9. No significant  
199 loss in the molecular weight was observed after 18 months at 4°C and 15°C. The molecular weight decrease  
200 from 123.6  $kg.mol^{-1}$  to 90.2  $kg.mol^{-1}$  after 18 months of immersion at 25°C. At 40°C the molecular weight  
201 decreases faster and is 36.1  $kg.mol^{-1}$  after 1 year of immersion. The decrease is even faster at 60°C and the



202 molecular weight falls to  $16.9 \text{ kg.mol}^{-1}$  after 3 months.

### 203 3.3. Initial and long term properties of the PBS/PBAT rope

#### 204 3.3.1. Initial characterization

205 Figure 11 presents the tensile/strain curves of tests on three ropes in the initial state. The initial stiffness  
206 measured between 1 kN and 5 kN was between 0.69 and 1.01 kN with a mean value of 0.83 kN. A mean  
207 strain at break and mean load at break were reproducible and respectively 28.6 kN and 35.2% with failure  
208 always observed at the end of one splice.

#### 209 3.3.2. Aged rope properties

210 Several rope samples were immersed in the same tanks as the monofilament samples at 15°C and 40°C to  
211 study the change in properties. At 15°C, one sample was removed and tested after 2, 4, 5, 9, and 12 months  
212 of immersion. At 40°C one sample was tested after 6 months of immersion and a second after 9 months.  
213 Figure 12 shows the residual strengths of the monofilament and the rope at 15°C and 40°C. No change in  
214 the load at break was observed for the rope immersed 1 year at 15°C. After 9 months at 40°C the rope broke  
215 at 17.1 kN, suggesting a loss of strength of 60%.

## 216 4. Discussion

217 This study aimed to investigate the natural seawater degradation of a PBS/PBAT marine rope, provid-  
218 ing insights into its performance during service and potential loss scenarios. The monofilament was first  
219 mechanically tested and compared with a commercial HDPE used in the fishing industry. The S-shaped  
220 curves obtained for the PBS/PBAT monofilament are typical of PBS monofilaments as seen in published  
221 studies (Kim et al., 2016, 2019; Grimaldo et al., 2020), with an increase in stiffness due to a strain induced  
222 crystallization as explained by Ichikawa et al. (1994). The overall properties of the PBS/PBAT monofilament  
223 are below those of HDPE, but Deroiné et al. (2019) showed that it was possible to greatly improve Young's  
224 modulus and stress at break of PBS monofilaments by optimising the drawing process. However, both  
225 monofilaments have similar loads and strains at break: 25.1 N and 34.5% respectively for the PBS/PBAT  
226 blend, and 21.4 N and 40.5% respectively for the HDPE, so the PBS/PBAT monofilament could already  
227 be considered as a substitute of HDPE in applications where the use of a slightly thicker monofilament is  
228 possible. PBS and PBAT are known for their biodegradability in soil and compost (Ahn et al., 2001; Tserki  
229 et al., 2006; Zhao et al., 2005), but their degradation in seawater is slower and less studied (Narancic et al.,  
230 2018). The monofilament may still lose its initial properties when exposed to a natural environment like  
231 seawater, so it was important to study these changes to determine if it can be used for marine applications  
232 such as fishing or aquaculture gear. Knowledge of the lifetime is also essential for Life Cycle Analysis (LCA),

233 in order to check the environmental benefits of a material change. The next step was therefore the study of  
234 seawater aged specimens.

235 The PBS/PBAT monofilament was immersed in renewed natural seawater tanks at different temper-  
236 atures alongside a commercial HDPE monofilament for comparison purpose. The loads at break of both  
237 monofilaments were monitored as an indicator of physical degradation. The HDPE monofilament's ability  
238 to retain its original properties after a 1-year immersion in seawater, regardless of temperature, explains  
239 its persistence in the marine environment and the potential threat it poses if discarded as a rope or fishing  
240 gear. The absence of property loss for the PBS/PBAT blend at 4°C and 15°C indicates that fishing gear  
241 made from this monofilament would have adequate durability for use in temperate waters, but also that it  
242 could persist in the environment and be a threat for at least 18 months if it is lost and sinks to low temper-  
243 ature regions of the ocean. On the other hand, the loss of properties in the PBS/PBAT monofilament at  
244 25°C is an indicator of the polymer's degradation in the marine environment, and fishing gear made from  
245 this filament would be less dangerous in case of loss. The rapid degradation of the breaking load at 40°C  
246 and 60°C indicates that the PBS/PBAT monofilament is much more susceptible to the marine environment  
247 and less stable than the HDPE monofilament. A detailed understanding of these degradations is therefore  
248 necessary, both to ensure that it does not lead to the formation of microplastics and also to account for this  
249 degradation in the design phase of the gear.

250 With regard to the loss of properties at 25°C, 40°C, and 60°C, various techniques have been used to  
251 identify the degradation mechanisms of the polymer. The surface morphology was first examined using a  
252 scanning electron microscope. No significant changes were observed at 4°C and 15°C which is consistent with  
253 the stability of the mechanical properties when immersed in seawater at these temperatures. The surface  
254 erosion pattern seen after 18 months at 25°C on Figure 7 was already observed on a PBSAT monofilament by  
255 [Kim et al. \(2016\)](#) in a natural environment at lower temperatures, after a longer time period of 2 years, and  
256 described to be a result from a biodegradation process. Surface erosion has also been observed on pure PBAT  
257 samples immersed in seawater for a 1 year period ([Kedzierski et al., 2018](#)). No surface erosion was seen after  
258 6 months in sterilized water while holes were presents after the same period and at the same temperature  
259 in the natural seawater tank as shown by Figure 8. The difference in erosion rates highlights the role of  
260 microorganisms present in natural seawater, which are absent in sterilized water. The observed surface  
261 degradation can be considered as an initial stage in a depolymerization process, triggered by enzymatically  
262 catalyzed hydrolysis, as described by [Müller et al. \(2001\)](#). This process could generate microbial assimilable  
263 intermediates. However, surface damage is not sufficient evidence to determine the overall assimilation of  
264 a polymer by microorganisms as [Zettler et al. \(2013\)](#) observed it on conventional plastics. Additionally,  
265 the absence of holes at lower temperatures indicates that further studies are necessary to fully understand  
266 the kinetics of this degradation. After 1 year at 40°C, no degradation justifying a 70% loss of properties  
267 was observed using the SEM. Nevertheless, the absence of holes at this temperature indicates that the

268 degradation is abiotic. For the sample immersed for 3 months at 60°C, lengthwise cracks were visible on  
269 the surface, corresponding to the material embrittlement as noted after the mechanical testing presented on  
270 Figure 4. As the surface morphologies were very different for the three temperatures where a significant loss of  
271 properties was measured, different degradation processes may be involved. Steric exclusion chromatography  
272 has been performed to further understand the loss of properties observed at the different temperatures.  
273 This technique provides information on the distribution in length of polymer chains within each sample.  
274 Polyester polymers like PBS and PBAT are known to be degraded by water by a chain scission process at  
275 the ester bonds (Bellenger et al., 1995; Deshouilles et al., 2022). The aim of using this method was to check  
276 whether the polymer chains were reducing in size during aging, and thus to confirm whether hydrolysis  
277 was one of the processes leading to the loss of properties of the samples at 25°C, 40°C, and 60°C. The  
278 absence of loss of molecular weight after 18 months at 4°C and 15°C on the Figure 9 correlates with the  
279 stability of the mechanical properties at these two temperatures as seen on the Figures 4 and 5. A significant  
280 reduction in polymer chain length was observed after 18 months at 25°C, indicating that hydrolysis is taking  
281 place and affecting the properties of the monofilament, in addition to surface erosion. At 40°C, the loss of  
282 molecular weight provides evidence of material degradation that was not visible through SEM observations  
283 alone. The decrease of molecular weight at 60°C could be considered as the potential cause of the visible  
284 cracks observed in the SEM photographs and the rapid loss of material properties visible on Figure 5. The  
285 decrease in molecular weight matches the temperature dependant loss of mechanical properties, so hydrolysis  
286 can be retained as one of the degradation processes taking place during the aging of the samples in seawater.  
287 Figure 10 presents the load at break versus the molecular weight and shows that a relation exists between  
288 these two properties. The data points obtained at 25°C are below the linear regression and yet they are still  
289 linear, which could be related to a lowering of the load at break introduced by the surface erosion seen on  
290 the SEM observations. The presence of multiple degradation processes at the same time does not allow a  
291 simple prediction of the lifespan of this polymer as done for other polymers in the literature (El-Mazry et al.,  
292 2012; Deshouilles et al., 2021; Dilkes-Hoffman et al., 2019). Modelling the loss of properties of biodegradable  
293 polymers at natural temperatures requires the separation of biotic and abiotic factors as shown by Deroiné  
294 (Deroiné, 2014).

295 The influence of the observed degradation processes has been investigated on the entire rope to determine  
296 whether the aging of the rope structure can be predicted from the loss of the monofilament's properties. The  
297 same methodology as for the monofilament has been used: initial characterization followed by monitoring  
298 the mechanical properties in natural seawater maintained at 15°C and 40°C.

299 Three samples has been tested for the initial state characterization. A similar mean strain at break to the  
300 monofilament, 35.2%, is obtained, with a strain-induced increase of the stiffness recorded at similar strains. If  
301 the rope were constructed ideally with no influence on the load distribution and each monofilament carrying  
302 an equal load, the load at break would be 33.4 kN, given that the rope is made of 1344 monofilaments.

303 However, the sample's load at break was measured to be 28.6 kN, which is 14% lower than the ideal case and  
304 expected due to the influence of rope construction and load introduction (splices) on the load distribution.  
305 Failure always occurred at the end of one of the splices, which is common for spliced ropes (Milne and  
306 McLaren, 2006). The braided structure of the rope resulted in a specific modulus that was 18% lower than  
307 that of the monofilament due to the construction angles of the rope. While the strain at break and load  
308 at break were reproducible between samples, a significant variability in stiffness was observed, which could  
309 be linked to manual splicing. The comparison between the properties of the rope and the monofilament  
310 suggests that this material is appropriate for producing twisted ropes.

311 After initial characterization, rope samples were immersed in natural seawater for a period up to 1 year  
312 at 15°C, and 9 months at 40°C. The absence of load loss in the rope sample after one year of immersion  
313 at 15°C seen on Figure 12 is consistent with the results obtained for the monofilament. At 40°C, the onset  
314 of property loss for the rope is delayed compared to the monofilament; however, once initiated, the rate of  
315 degradation appears to be similar, as the slopes are comparable. The delay observed at this temperature  
316 could be caused by two phenomena : (i) the monofilament testing is more severe, with the tensile test clamps  
317 causing lower break loads than the splices, (ii) the water diffusion is slower in the rope and the hydrolysis  
318 observed on Figure 9 is not homogeneous between all monofilaments.

319 In order to use this type of new monofilament in a net twine or rope it is necessary to account for  
320 the changes in properties with time at the design phase. This requires the use of a model which can  
321 integrate material property changes and analyze their influence on the structure. In the fishing industry,  
322 that structure is often in the form of a braid, whether net twine or larger braided ropes. Finite element  
323 modelling may be used, particularly if the full net structure including knots is to be studied, but here the  
324 focus is at the rope level. FRM, a modelling tool developed to predict rope properties, is therefore more  
325 appropriate. It has been used successfully for previous studies on large marine ropes (Davies et al., 2006)  
326 and can predict tensile properties and tension-twist coupling. The input data are the sub-element properties  
327 (the monofilament load-strain plots here) and their geometry within the rope structure.

328 The load-strain properties of the monofilaments (Figure 3) were used to estimate the initial unaged rope  
329 properties. The input data are normalized with respect to break load and strain and modelled using a  
330 polynomial fit as depicted by Figure 13. Given the highly non-linear behaviour a 6th degree polynomial fit  
331 was required for unaged specimens.

332 As there was some variability in monofilament properties the two extreme curves (on Figure 3) were also  
333 examined. The rope model offers two options, hard and soft constructions. The latter is usually applied  
334 to multifilament yarns, which can deform under loading; the monofilaments show higher transverse rigidity  
335 and a hard option was chosen. The numbers and orientations of the filaments are then entered and the  
336 model provides a load-strain plot for the unaged rope for each set of monofilament properties, Figure 14.

337 The predicted break loads, between 23 and 28.6 kN, are quite close to the measured unaged rope values

338 as shown in Table 2. The strains at break are also similar, but the overall behavior of the model is less  
339 linear than the rope due to the high order polynomials used to fit the monofilament curves. These results  
340 indicate that the model provides a satisfactory prediction of braided rope properties, so it was then applied  
341 to the aged ropes. After aging at 15°C there was no drop in measured monofilament properties even after  
342 12 months in seawater, so only the 40°C condition is described here.

343 The same method as for the initial state has been used to predict the rope properties after aging from  
344 the aged monofilament load-strain curves and polynomial fits. Once again load at break and initial stiffness  
345 values were measured, and these are given in Table 2, which summarizes the model results. Figure 15 shows  
346 the prediction of aging of the rope alongside the change in properties for the monofilament and the rope.

347 For the unaged samples the prediction based on the mean monofilament properties is within 10% of  
348 the measured value; when the maximum measured break load is used the prediction is even closer. For  
349 the samples after immersion, the model tends to overestimate the effect of aging on failure properties,  
350 providing a conservative break load value. This is an interesting result. The model assumption is that all  
351 the monofilaments degrade to the same extent as an individual monofilament exposed to the same aging  
352 conditions. However, monofilaments within a strand will be more or less protected from degradation due to  
353 the limited access of bacteria to the interior of the rope construction. For smaller ropes or net twines, the  
354 prediction may be closer to measured values.

## 355 5. Conclusion

356 This study investigated the potential use of a PBS/PBAT blend to mitigate the environmental impact  
357 of lost marine ropes. Although the PBS/PBAT monofilament had lower properties than HDPE, this could  
358 be compensated by increasing the diameter. Both types of monofilament were aged in natural seawater  
359 at various temperatures for at least one year. The HDPE monofilament showed no loss of mechanical  
360 strength, whereas the PBS/PBAT monofilament experienced degradation via hydrolysis and biodegradation  
361 at 25°C, 40°C, and 60°C. While PBS/PBAT monofilament may be a safer option due to its lower persistence  
362 in the marine environment, further research is needed to decouple the degradation mechanisms, enhance  
363 understanding of their kinetics, and develop models for predicting the lifespan of such materials.

364 Additionally, the rope made from this PBS/PBAT monofilament was immersed in the same conditions  
365 to evaluate aging within a complex arrangement of monofilaments and determine if the loss of properties  
366 could be predicted from the monofilament data using the FRM modelling tool. The rope's loss of properties  
367 was slower than that of the monofilament, and while the initial correlation was good, the modelling tool  
368 predicted a faster loss of properties. The conservative results may be due to a more severe mechanical test  
369 conditions for the aged monofilament or a degradation gradient within the rope structure. Nonetheless, the  
370 FRM provided an effective approach to assess initial rope properties and provide a conservative prediction

371 of aging states.

372 This study provides seawater aging data for a biodegradable rope that could help reduce the environ-  
373 mental impact of synthetic ropes at sea. However, it should be noted that short-term impact cannot be  
374 completely avoided (Wilcox and Hardesty, 2016), and this material should be used in conjunction with  
375 existing solutions to produce safer ropes for marine wildlife and to help reduce open sea plastic pollution.  
376 Overall, the use of biodegradable rope such as the one evaluated in this study shows promise in addressing  
377 the issue of plastic pollution in the world's oceans and represents an important step towards sustainable  
378 marine practices.

### 379 **CRedit authorship contribution statement**

380 Louis Le Gué: Conceptualization, data gathering and investigation, formal analysis, visualization, writing  
381 – original draft, writing - review and editing.

382 Peter Davies: Conceptualization, data gathering and investigation, formal analysis, writing – original  
383 draft, writing - review and editing.

384 Mael Arhant: Conceptualization, investigation, formal analysis, writing - review and editing.

385 Benoit Vincent: Conceptualization, investigation, writing - review and editing.

386 Erwan Tanguy: Conceptualization, investigation, writing - review and editing.

### 387 **Declaration of competing interest**

388 The authors declare that they have no known competing financial interests or personal relationships that  
389 could have appeared to influence the work reported in this paper.

### 390 **Acknowledgements**

391 The authors would like to thank Nicolas Lacotte for his help with splicing and tests on ropes, and Nicolas  
392 Gayet for providing the SEM images and his expertise in the use of the scanning electron microscope.

Property	PBS/PBAT	HDPE
Density [ $g.cm^{-3}$ ]	1.25	0.95
Diameter [mm]	0.35	0.28
Tex [ $g.km^{-1}$ ]	121.7	54.6
Young's Modulus [GPa]	0.79	1.90
Load at break [N]	25.1	21.4
Stress at break [MPa]	261	368
Strain at break [%]	34.5	40.5

Table 1: Properties of the PBS/PBAT blend and the commercial HDPE.

Condition	Initial stiffness [kN]	Break load [kN]	
	Experimental (Min-Max)	Experimental (Min-Max)	Model (Min-Max)
Unaged	0.83	28.6	26.3
	(0.69 - 1.01)	(28.5 - 28.7)	(23.1 - 28.9)
15°C, 12 months	0.69	29.1	25.3 (23.9 - 26.0)
40°C, 6 months	0.64	25.4	17.4 (16.2 - 19.4)
40°C, 9 months	0.64	17.0	10.6 (8.1 - 12.7)

Table 2: Summary of main rope model results and predictions.

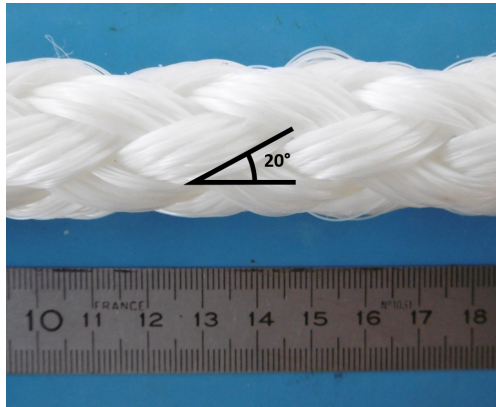


Figure 1: Close up view of the rope construction.



Figure 2: Rope tensile testing set-up equipped with cameras for strain measurements.

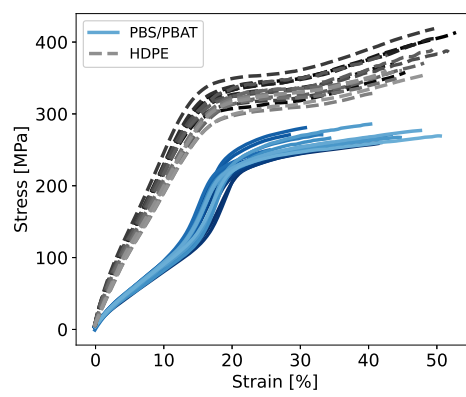


Figure 3: Tensile test curves at the initial state for the PBS/PBAT blend and HDPE.



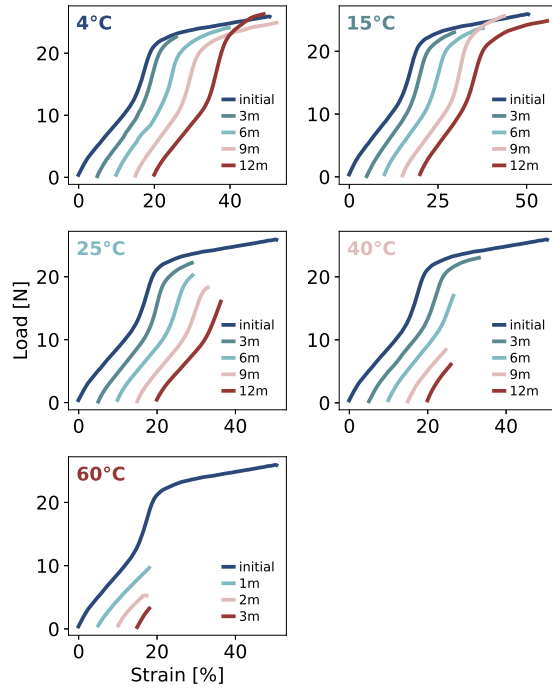


Figure 4: Change in the tensile test curve with aging at different temperatures.

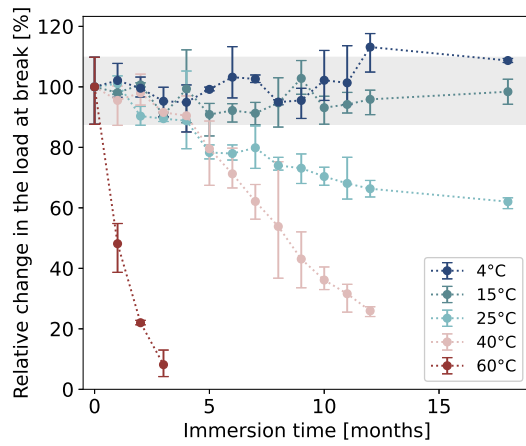


Figure 5: Load at break loss depending on the immersion time at different temperatures.

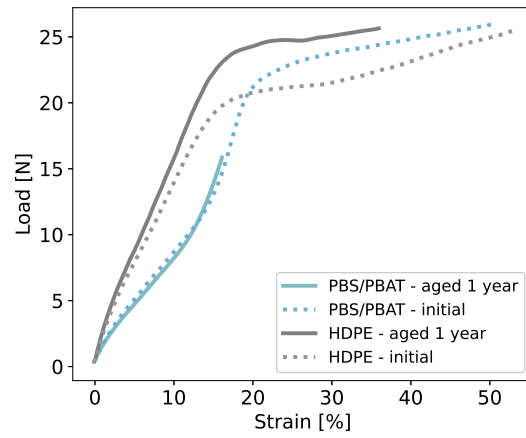


Figure 6: Tensile test curves after 1 year immersed at 25°C for the PBS/PBAT blend and HDPE.

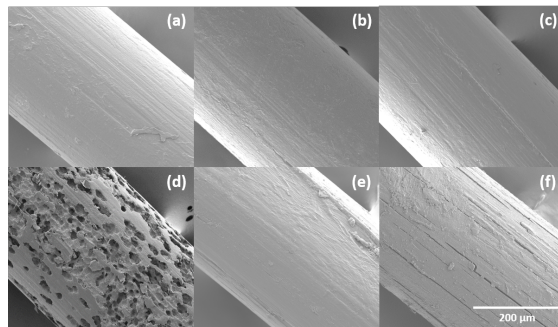


Figure 7: Surface observations for different immersion times and temperatures : (a) initial sample (b) after 18 months at 4°C, (c) after 18 months at 15°C, (d) after 18 months at 25°C, (e) after 12 months at 40°C, (f) after 3 months at 60°C.

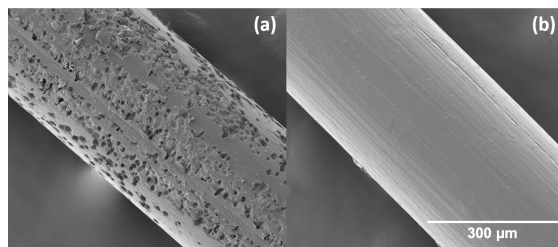


Figure 8: Surface observations for PBS/PBAT monofilaments immersed 6 months in (a) natural seawater and (b) deionized and sterilized water.

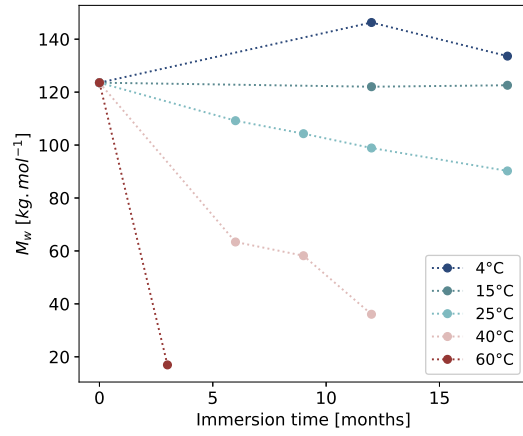


Figure 9:  $M_w$  change depending on the immersion time.

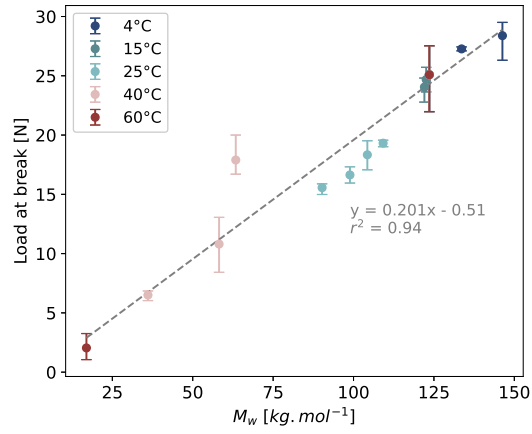


Figure 10: Load at break versus molecular weight  $M_w$ .

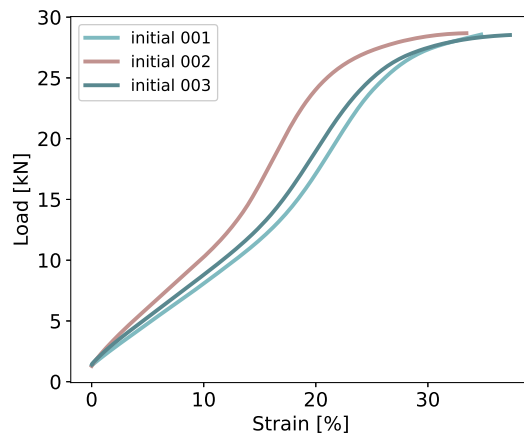


Figure 11: Tensile test curves of 3 rope samples before aging.

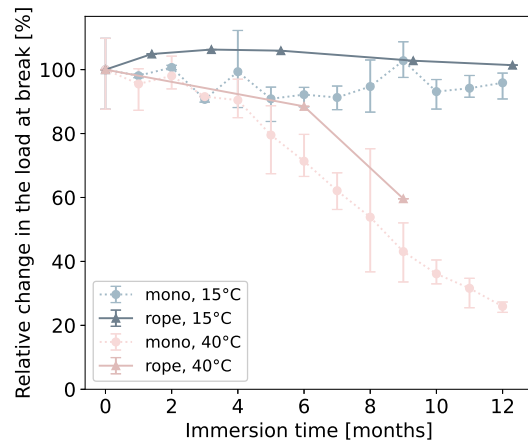


Figure 12: Load at break change for monofilament and rope at 15°C and 40°C.

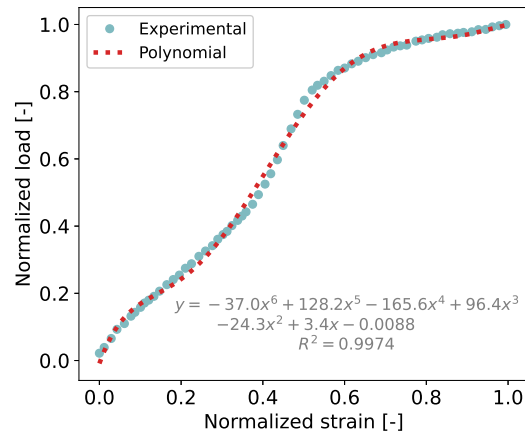


Figure 13: Example of monofilament input mean data for FRM.

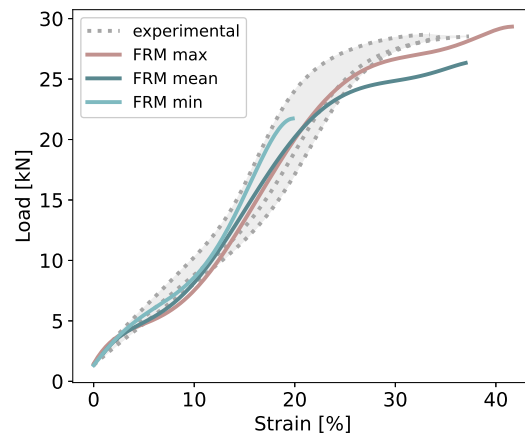


Figure 14: Predicted load-strain behaviour, unaged rope.

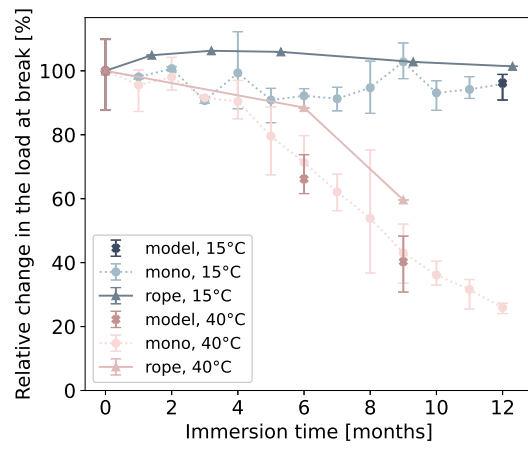


Figure 15: Load at break estimations predicted by the model alongside load at break for monofilament and rope at 15°C and 40°C.

## 393 References

- 394 Adhikari, D., Mukai, M., Kubota, K., Kai, T., Kaneko, N., Araki, K.S., Kubo, M., 2016. Degradation of Bioplastics in Soil  
395 and Their Degradation Effects on Environmental Microorganisms. *Journal of Agricultural Chemistry and Environment* 05,  
396 23. URL: <http://www.scirp.org/journal/PaperInformation.aspx?PaperID=64039&#abstract>, doi:10.4236/jacen.2016.  
397 51003. number: 01 Publisher: Scientific Research Publishing.
- 398 Ahn, B.D., Kim, S.H., Kim, Y.H., Yang, J.S., 2001. Synthesis and characterization of the biodegradable copolymers from  
399 succinic acid and adipic acid with 1,4-butanediol. *Journal of Applied Polymer Science* 82, 2808–2826. URL: [https://  
400 onlinelibrary.wiley.com/doi/abs/10.1002/app.2135](https://onlinelibrary.wiley.com/doi/abs/10.1002/app.2135), doi:10.1002/app.2135.
- 401 Bagheri, A., Laforsch, C., Greiner, A., Agarwal, S., 2017. Fate of So-Called Biodegradable Polymers in Seawater and Freshwater.  
402 *Global Challenges* 1, 1700048. doi:10.1002/gch2.201700048.
- 403 Banfield, S., Hearle, J.W.S., Leech, C.M., Lawrence, C.A., 2001. Fibre Rope Modeller (FRM) : A CAD program for the  
404 Performance Prediction of Advanced Cords and Ropes under Complex Loading Environments. Technical Report. Tension  
405 Technology International.
- 406 Bellenger, V., Ganem, M., Mortaigne, B., Verdu, J., 1995. Lifetime prediction in the hydrolytic ageing of polyesters. *Polymer*  
407 *Degradation and Stability* 49, 91–97. URL: <https://www.sciencedirect.com/science/article/pii/014139109500049R>,  
408 doi:10.1016/0141-3910(95)00049-R.
- 409 Brakstad, O.G., Sørensen, L., Hakvåg, S., Føre, H.M., Su, B., Aas, M., Ribicic, D., Grimaldo, E., 2022. The fate of conventional  
410 and potentially degradable gillnets in a seawater-sediment system. *Marine Pollution Bulletin* 180, 113759. URL: [https://  
411 //www.sciencedirect.com/science/article/pii/S0025326X22004416](https://www.sciencedirect.com/science/article/pii/S0025326X22004416), doi:10.1016/j.marpolbul.2022.113759.
- 412 Carbery, M., O'Connor, W., Palanisami, T., 2018. Trophic transfer of microplastics and mixed contaminants in the marine  
413 food web and implications for human health. *Environment International* 115, 400–409. URL: [https://www.sciencedirect.  
414 com/science/article/pii/S0160412017322298](https://www.sciencedirect.com/science/article/pii/S0160412017322298), doi:10.1016/j.envint.2018.03.007.
- 415 Cerbule, K., Grimaldo, E., Herrmann, B., Larsen, R.B., Brčić, J., Vollstad, J., 2022a. Can biodegradable materials reduce  
416 plastic pollution without decreasing catch efficiency in longline fishery? *Marine Pollution Bulletin* 178. doi:10.1016/j.  
417 marpolbul.2022.113577.
- 418 Cerbule, K., Herrmann, B., Grimaldo, E., Larsen, R.B., Savina, E., Vollstad, J., 2022b. Comparison of the efficiency and modes  
419 of capture of biodegradable versus nylon gillnets in the Northeast Atlantic cod (*Gadus morhua*) fishery. *Marine Pollution*  
420 *Bulletin* 178. doi:10.1016/j.marpolbul.2022.113618.
- 421 Davies, P., Bouquet, P., Conte, M., Deuff, A., 2006. Tension/Torsion Behavior of Deepwater Synthetic Mooring Lines, in:  
422 *Offshore Technology Conference, Offshore Technology Conference, Houston, Texas, USA*. URL: [http://www.onepetro.org/  
423 doi/10.4043/17872-MS](http://www.onepetro.org/doi/10.4043/17872-MS), doi:10.4043/17872-MS.
- 424 De Monte, C., Locritani, M., Merlino, S., Ricci, L., Pistolesi, A., Bronco, S., 2022. An In Situ Experiment to Evaluate the  
425 Aging and Degradation Phenomena Induced by Marine Environment Conditions on Commercial Plastic Granules. *Polymers*  
426 14, 1111. URL: <https://www.mdpi.com/2073-4360/14/6/1111>, doi:10.3390/polym14061111.
- 427 De Munck, N.A., 1980. Gas phase hydroformylation of propylene and allyl alcohol with immobilized  
428 rhodium complexes. Delft University Press URL: [https://repository.tudelft.nl/islandora/object/uuid/  
429 3Ad0a9ff72-99ad-4767-922a-e9a80aee5a6](https://repository.tudelft.nl/islandora/object/uuid%3Ad0a9ff72-99ad-4767-922a-e9a80aee5a6). publisher: Delft University Press.
- 430 Delacuvellerie, A., Brusselman, A., Cyriaque, V., Benali, S., Moins, S., Raquez, J.M., Gobert, S., Wattiez, R., 2023. Long-  
431 term immersion of compostable plastics in marine aquarium: Microbial biofilm evolution and polymer degradation. *Marine*  
432 *Pollution Bulletin* 189, 114711. URL: <https://www.sciencedirect.com/science/article/pii/S0025326X2300142X>, doi:10.  
433 1016/j.marpolbul.2023.114711.
- 434 Deroiné, M., 2014. Étude du vieillissement de biopolymères en milieu marin. PhD thesis. Université de Bretagne Sud. URL:  
435 <https://tel.archives-ouvertes.fr/tel-01193329>.

436 Deroiné, M., César, G., Le Duigou, A., Davies, P., Bruzaud, S., 2015. Natural Degradation and Biodegradation of Poly(3-  
437 Hydroxybutyrate-co-3-Hydroxyvalerate) in Liquid and Solid Marine Environments. *Journal of Polymers and the Environment*  
438 23, 493–505. URL: <http://link.springer.com/10.1007/s10924-015-0736-5>, doi:10.1007/s10924-015-0736-5.

439 Deroiné, M., Pillin, I., Le Maguer, G., Chauvel, M., Grohens, Y., 2019. Development of new generation fishing gear: A resistant  
440 and biodegradable monofilament. *Polymer Testing* 74, 163–169. URL: <https://www.sciencedirect.com/science/article/pii/S0142941818311711>, doi:10.1016/j.polymertesting.2018.11.039.

442 Deshoules, Q., Gall, M.L., Benali, S., Raquez, J.M., Dreanno, C., Arhant, M., Priour, D., Cerantola, S., Stoclet, G.,  
443 Gac, P.Y.L., 2022. Hydrolytic degradation of biodegradable poly(butylene adipate-co-terephthalate) (PBAT) - To-  
444 wards an understanding of microplastics fragmentation. *Polymer Degradation and Stability* 205, 110122. URL: <https://www.sciencedirect.com/science/article/pii/S0141391022003007>, doi:10.1016/j.polymdegradstab.2022.110122.

446 Deshoules, Q., Le Gall, M., Dreanno, C., Arhant, M., Priour, D., Le Gac, P.Y., 2021. Modelling pure polyamide 6 hydrolysis:  
447 Influence of water content in the amorphous phase. *Polymer Degradation and Stability* 183, 109435. URL: <https://www.sciencedirect.com/science/article/pii/S0141391020303645>, doi:10.1016/j.polymdegradstab.2020.109435.

449 Dilkes-Hoffman, L.S., Lant, P.A., Laycock, B., Pratt, S., 2019. The rate of biodegradation of PHA bioplastics in the marine en-  
450 vironment: A meta-study. *Marine Pollution Bulletin* 142, 15–24. URL: <https://www.sciencedirect.com/science/article/pii/S0025326X19302048>, doi:10.1016/j.marpolbul.2019.03.020.

452 Doi, Y., Kanesawa, Y., Kunioka, M., Saito, T., 1990. Biodegradation of microbial copolyesters: poly(3-hydroxybutyrate-co-3-  
453 hydroxyvalerate) and poly(3-hydroxybutyrate-co-4-hydroxybutyrate). *Macromolecules* 23, 26–31. URL: <https://doi.org/10.1021/ma00203a006>, doi:10.1021/ma00203a006. publisher: American Chemical Society.

455 El-Mazry, C., Correc, O., Colin, X., 2012. A new kinetic model for predicting polyamide 6-6 hydrolysis and its mechanical  
456 embrittlement. *Polymer Degradation and Stability* 97, 1049–1059. URL: <https://linkinghub.elsevier.com/retrieve/pii/S014139101200081X>, doi:10.1016/j.polymdegradstab.2012.03.003.

458 European Bioplastics e.V., 2020. Bioplastics market data. URL: <https://www.european-bioplastics.org/market/>.

459 Ferreira, F.V., Cividanes, L.S., Gouveia, R.F., Lona, L.M., 2019. An overview on properties and appli-  
460 cations of poly(butylene adipate-co-terephthalate)–PBAT based composites. *Polymer Engineering & Science*  
461 59, E7–E15. URL: <https://onlinelibrary.wiley.com/doi/abs/10.1002/pen.24770>, doi:10.1002/pen.24770. eprint:  
462 <https://onlinelibrary.wiley.com/doi/pdf/10.1002/pen.24770>.

463 Freyermouth, F., 2014. Etude et modification des propriétés du poly(butylène succinate), un polyester biosourcé et  
464 biodégradable. PhD thesis. INSA Lyon. URL: <https://tel.archives-ouvertes.fr/tel-01135306>.

465 Furuike, T., Nagahama, H., Chaochai, T., Tamura, H., 2015. Preparation and Characterization of Chitosan-Coated Poly(l-  
466 Lactic Acid) Fibers and Their Braided Rope. *Fibers* 3, 380–393. URL: <http://www.mdpi.com/2079-6439/3/4/380>, doi:10.  
467 3390/fib3040380.

468 Galgani, F., Pham, C.K., Claro, F., Consoli, P., 2018. Marine animal forests as useful indicators of entanglement by marine litter.  
469 *Marine Pollution Bulletin* 135, 735–738. URL: <https://www.sciencedirect.com/science/article/pii/S0025326X1830568X>,  
470 doi:10.1016/j.marpolbul.2018.08.004.

471 Grimaldo, E., Herrmann, B., Jacques, N., Kubowicz, S., Cerbule, K., Su, B., Larsen, R., Vollstad, J., 2020. The effect  
472 of long-term use on the catch efficiency of biodegradable gillnets. *Marine Pollution Bulletin* 161, 111823. URL: <https://www.sciencedirect.com/science/article/pii/S0025326X20309413>, doi:10.1016/j.marpolbul.2020.111823.

474 Grimaldo, E., Herrmann, B., Su, B., Føre, H.M., Vollstad, J., Olsen, L., Larsen, R.B., Tatone, I., 2019. Comparison of  
475 fishing efficiency between biodegradable gillnets and conventional nylon gillnets. *Fisheries Research* 213, 67–74. URL:  
476 <https://www.sciencedirect.com/science/article/pii/S0165783619300037>, doi:10.1016/j.fishres.2019.01.003.

477 Grimaldo, E., Herrmann, B., Tveit, G.M., Vollstad, J., Schei, M., 2018a. Effect of Using Biodegradable Gill Nets on the Catch  
478 Efficiency of Greenland Halibut. *Marine and Coastal Fisheries* 10, 619–629. URL: <https://afspubs.onlinelibrary.wiley>.

479 [com/doi/full/10.1002/mcf2.10058](https://doi.org/10.1002/mcf2.10058), doi:10.1002/mcf2.10058. publisher: John Wiley & Sons, Ltd.

480 Grimaldo, E., Herrmann, B., Vollstad, J., Su, B., Moe Føre, H., Larsen, R.B., Tatone, I., 2018b. Fishing efficiency of  
481 biodegradable PBSAT gillnets and conventional nylon gillnets used in Norwegian cod (*Gadus morhua*) and saithe (*Pollachius*  
482 *virens*) fisheries. *ICES Journal of Marine Science* 75, 2245–2256. URL: <https://doi.org/10.1093/icesjms/fsy108>, doi:10.  
483 [1093/icesjms/fsy108](https://doi.org/10.1093/icesjms/fsy108).

484 Harris, N., Dennis, A.J., Harrison, G.E., 1980. Production of butane-1,4-diol, EP patent 0018163, assigned to Davy-McKee Oil  
485 & Chemicals Ltd. URL: <https://patentimages.storage.googleapis.com/a4/7c/7e/68b77a836d331f/EP0018163A1.pdf>.

486 Huang, D., Hu, Z.D., Liu, T.Y., Lu, B., Zhen, Z.C., Wang, G.X., Ji, J.H., 2020. Seawater degradation of PLA accelerated by  
487 water-soluble PVA. *e-Polymers* 20, 759–772. URL: [https://www.degruyter.com/document/doi/10.1515/epoly-2020-0071/](https://www.degruyter.com/document/doi/10.1515/epoly-2020-0071/html)  
488 [html](https://www.degruyter.com/document/doi/10.1515/epoly-2020-0071/html), doi:10.1515/epoly-2020-0071. publisher: De Gruyter.

489 Ichikawa, Y., Suzuki, J., Washiyama, J., Moteki, Y., Noguchi, K., Okuyama, K., 1994. Strain-induced crystal modification  
490 in poly(tetramethylene succinate). *Polymer* 35, 3338–3339. URL: [https://www.sciencedirect.com/science/article/pii/](https://www.sciencedirect.com/science/article/pii/S002386194901449)  
491 [002386194901449](https://www.sciencedirect.com/science/article/pii/S002386194901449), doi:10.1016/0032-3861(94)90144-9.

492 Jian, J., Xiangbin, Z., Xianbo, H., 2020. An overview on synthesis, properties and applications of poly(butylene-adipate-co-  
493 terephthalate)–PBAT. *Advanced Industrial and Engineering Polymer Research* 3, 19–26. URL: [https://www.sciencedirect.](https://www.sciencedirect.com/science/article/pii/S2542504820300014)  
494 [com/science/article/pii/S2542504820300014](https://www.sciencedirect.com/science/article/pii/S2542504820300014), doi:10.1016/j.aiepr.2020.01.001.

495 Johnson, A., Salvador, G., Kenney, J., Robbins, J., Kraus, S., Landry, S., Clapham, P., 2005. Fishing Gear Involved in  
496 Entanglements of Right and Humpback Whales. *Marine Mammal Science* 21, 635–645. URL: [https://onlinelibrary.](https://onlinelibrary.wiley.com/doi/abs/10.1111/j.1748-7692.2005.tb01256.x)  
497 [wiley.com/doi/abs/10.1111/j.1748-7692.2005.tb01256.x](https://onlinelibrary.wiley.com/doi/abs/10.1111/j.1748-7692.2005.tb01256.x), doi:10.1111/j.1748-7692.2005.tb01256.x.

498 Kedzierski, M., D’Almeida, M., Magueresse, A., Le Grand, A., Duval, H., César, G., Sire, O., Bruzard, S., Le Tilly,  
499 V., 2018. Threat of plastic ageing in marine environment. Adsorption/desorption of micropollutants. *Marine Pollution*  
500 *Bulletin* 127, 684–694. URL: <https://www.sciencedirect.com/science/article/pii/S0025326X17310925>, doi:10.1016/j.  
501 [marpolbul.2017.12.059](https://www.sciencedirect.com/science/article/pii/S0025326X17310925).

502 Kim, S., Kim, P., Jeong, S., Bae, J., Lim, J., Oh, W., 2018. Fishing performance of a coastal drift net in accordance with  
503 materials of the environmentally-friendly biodegradable net twine. *Journal of the Korean Society of Fisheries Technology*  
504 54, 97–106. URL: <http://ksft.or.kr/journal/article.php?code=61680>, doi:10.3796/KSFOT.2018.54.2.097.

505 Kim, S., Kim, P., Lim, J., An, H., Suuronen, P., 2016. Use of biodegradable driftnets to prevent ghost fishing: physical  
506 properties and fishing performance for yellow croaker. *Animal Conservation* 19, 309–319. URL: [https://onlinelibrary.](https://onlinelibrary.wiley.com/doi/10.1111/acv.12256)  
507 [wiley.com/doi/10.1111/acv.12256](https://onlinelibrary.wiley.com/doi/10.1111/acv.12256), doi:10.1111/acv.12256.

508 Kim, S.H., Kim, P., Jeong, S.J., Lee, K., Oh, W., 2019. Physical Properties of Biodegradable Fishing Net in Accordance with  
509 Heat-Treatment Conditions for Reducing Ghost Fishing. *Turkish Journal of Fisheries and Aquatic Sciences* 20, 127–135.  
510 URL: [https://www.semanticscholar.org/paper/Physical-Properties-of-Biodegradable-Fishing-Net-in-Kim-Kim/](https://www.semanticscholar.org/paper/Physical-Properties-of-Biodegradable-Fishing-Net-in-Kim-Kim/aa4f274fe257f545de6ae241c6c9fd6b6e014ff2)  
511 [aa4f274fe257f545de6ae241c6c9fd6b6e014ff2](https://www.semanticscholar.org/paper/Physical-Properties-of-Biodegradable-Fishing-Net-in-Kim-Kim/aa4f274fe257f545de6ae241c6c9fd6b6e014ff2).

512 Knowlton, A., Hamilton, P., Marx, M., Pettis, H., Kraus, S., 2012. Monitoring North Atlantic right whale *Eubalaena glacialis*  
513 entanglement rates: a 30 yr retrospective. *Marine Ecology Progress Series* 466, 293–302. URL: [http://www.int-res.com/](http://www.int-res.com/abstracts/meps/v466/p293-302/)  
514 [abstracts/meps/v466/p293-302/](http://www.int-res.com/abstracts/meps/v466/p293-302/), doi:10.3354/meps09923.

515 Knowlton, A.R., Robbins, J., Landry, S., McKenna, H.A., Kraus, S.D., Werner, T.B., 2016. Effects of fishing rope strength on  
516 the severity of large whale entanglements. *Conservation Biology* 30, 318–328. URL: [https://onlinelibrary.wiley.com/](https://onlinelibrary.wiley.com/doi/abs/10.1111/cobi.12590)  
517 [doi/abs/10.1111/cobi.12590](https://onlinelibrary.wiley.com/doi/abs/10.1111/cobi.12590), doi:10.1111/cobi.12590.

518 Kraus, S., Fasick, J., Werner, T., McFarron, P., 2014. Enhancing the Visibility of Fishing Ropes to Reduce Right Whale  
519 Entanglements. Technical Report. New England Aquarium Corporation.

520 Le Gall, M., Niu, Z., Curto, M., Catarino, A.I., Demeyer, E., Jiang, C., Dhakal, H., Everaert, G., Davies, P., 2022. Behaviour  
521 of a self-reinforced polylactic acid (SRPLA) in seawater. *Polymer Testing* 111, 107619. URL: <https://www.sciencedirect.com/doi/abs/10.1016/j.polymtest.2022.107619>.



522 [com/science/article/pii/S0142941822001441](https://doi.org/10.1016/j.polymertesting.2022.107619), doi:10.1016/j.polymertesting.2022.107619.

523 Luzier, W.D., 1992. Materials derived from biomass/biodegradable materials. *Proceedings of the National Academy of Sciences*

524 89, 839–842. URL: <https://www.pnas.org/content/89/3/839>, doi:10.1073/pnas.89.3.839. publisher: National Academy

525 of Sciences Section: Research Article.

526 Martin, R.T., Camargo, L.P., Miller, S.A., 2014. Marine-degradable polylactic acid. *Green Chemistry* 16, 1768–1773. URL:

527 <https://pubs.rsc.org/en/content/articlelanding/2014/gc/c3gc42604a>, doi:10.1039/C3GC42604A. publisher: The Royal

528 Society of Chemistry.

529 de Matos Costa, A.R., Crocitti, A., Hecker de Carvalho, L., Carroccio, S.C., Cerruti, P., Santagata, G., 2020. Properties

530 of Biodegradable Films Based on Poly(butylene Succinate) (PBS) and Poly(butylene Adipate-co-Terephthalate) (PBAT)

531 Blends. *Polymers* 12, 2317. URL: <https://www.mdpi.com/2073-4360/12/10/2317>, doi:10.3390/polym12102317. number: 10

532 Publisher: Multidisciplinary Digital Publishing Institute.

533 Milne, K.A., McLaren, A.J., 2006. An assessment of the strength of knots and splices used as eye terminations in a sailing

534 environment. *Sports Engineering* 9, 1–13. URL: <http://link.springer.com/10.1007/BF02844258>, doi:10.1007/BF02844258.

535 Moore, M.J., Bogomolni, A., Bowman, R., Hamilton, P.K., Harry, C.T., Knowlton, A.R., Landry, S., Rotstein, D.S., Touhey, K.,

536 2006. Fatally entangled right whales can die extremely slowly, in: *OCEANS 2006*, pp. 1–3. doi:10.1109/OCEANS.2006.306792.

537 ISSN: 0197-7385.

538 Morales-Caselles, C., Viejo, J., Martí, E., González-Fernández, D., Pragnell-Raasch, H., González-Gordillo, J.I., Montero, E.,

539 Arroyo, G.M., Hanke, G., Salvo, V.S., Basurko, O.C., Mallos, N., Lebreton, L., Echevarría, F., van Emmerik, T., Duarte,

540 C.M., Gálvez, J.A., van Sebille, E., Galgani, F., García, C.M., Ross, P.S., Bartual, A., Ioakeimidis, C., Markalain, G., Isobe,

541 A., Cózar, A., 2021. An inshore–offshore sorting system revealed from global classification of ocean litter. *Nature Sustain-*

542 *ability* 4, 484–493. URL: <http://www.nature.com/articles/s41893-021-00720-8>, doi:10.1038/s41893-021-00720-8.

543 Możejko-Ciesielska, J., Kiewisz, R., 2016. Bacterial polyhydroxyalkanoates: Still fabulous? *Microbiological Research* 192,

544 271–282. URL: <https://www.sciencedirect.com/science/article/pii/S094450131630043X>, doi:10.1016/j.micres.2016.

545 07.010.

546 Müller, R.J., Kleeberg, I., Deckwer, W.D., 2001. Biodegradation of polyesters containing aromatic constituents. *Journal of*

547 *Biotechnology* 86, 87–95. URL: <https://www.sciencedirect.com/science/article/pii/S0168165600004077>, doi:10.1016/

548 S0168-1656(00)00407-7.

549 Nakayama, A., Yamano, N., Kawasaki, N., 2019. Biodegradation in seawater of aliphatic polyesters. *Polymer Degradation and*

550 *Stability* 166, 290–299. URL: <https://www.sciencedirect.com/science/article/pii/S0141391019302071>, doi:10.1016/j.

551 [polydegradstab.2019.06.006](https://doi.org/10.1016/j.polydegradstab.2019.06.006).

552 Narancic, T., Verstichel, S., Reddy Chaganti, S., Morales-Gamez, L., Kenny, S.T., De Wilde, B., Babu Padamati, R., O'Connor,

553 K.E., 2018. Biodegradable Plastic Blends Create New Possibilities for End-of-Life Management of Plastics but They Are

554 Not a Panacea for Plastic Pollution. *Environmental Science & Technology* 52, 10441–10452. URL: [https://doi.org/10.](https://doi.org/10.1021/acs.est.8b02963)

555 [1021/acs.est.8b02963](https://doi.org/10.1021/acs.est.8b02963), doi:10.1021/acs.est.8b02963. publisher: American Chemical Society.

556 Numata, K., Abe, H., Iwata, T., 2009. Biodegradability of Poly(hydroxyalkanoate) Materials. *Materials* 2, 1104–1126. URL:

557 <http://www.mdpi.com/1996-1944/2/3/1104>, doi:10.3390/ma2031104.

558 Puchalski, M., Kwolek, S., Szparaga, G., Chrzanowski, M., Krucińska, I., 2017. Investigation of the Influence of PLA Molecular

559 Structure on the Crystalline Forms ( $\alpha'$  and  $\alpha$ ) and Mechanical Properties of Wet Spinning Fibres. *Polymers* 9, 18. URL:

560 <http://www.mdpi.com/2073-4360/9/1/18>, doi:10.3390/polym9010018.

561 Rheinberger, T., Wolfs, J., Paneth, A., Gojzewski, H., Paneth, P., Wurm, F.R., 2021. RNA-Inspired and Acceler-

562 ated Degradation of Polylactide in Seawater. *Journal of the American Chemical Society* 143, 16673–16681. URL:

563 <https://pubs.acs.org/doi/10.1021/jacs.1c07508>, doi:10.1021/jacs.1c07508.

564 Saito, Y., Doi, Y., 1994. Microbial synthesis and properties of poly(3-hydroxybutyrate-co-4-hydroxybutyrate) in Coma-

565 monas acidovorans. *International Journal of Biological Macromolecules* 16, 99–104. URL: <https://www.sciencedirect.com/science/article/pii/S0141813094900221>, doi:10.1016/0141-8130(94)90022-1.

566

567 Samadi, K., Francisco, M., Hegde, S., Diaz, C.A., Trabold, T.A., Dell, E.M., Lewis, C.L., 2019. Mechanical, rheological  
568 and anaerobic biodegradation behavior of a Poly(lactic acid) blend containing a Poly(lactic acid)-co-poly(glycolic acid)  
569 copolymer. *Polymer Degradation and Stability* 170, 109018. URL: <https://www.sciencedirect.com/science/article/pii/S0141391019303465>, doi:10.1016/j.polymdegradstab.2019.109018.

570

571 Savenkova, L., Gercberga, Z., Nikolaeva, V., Dzene, A., Bibers, I., Kalnin, M., 2000. Mechanical properties and biodegradation  
572 characteristics of PHB-based films. *Process Biochemistry* 35, 573–579. URL: <https://www.sciencedirect.com/science/article/pii/S0032959299001077>, doi:10.1016/S0032-9592(99)00107-7.

573

574 Sekiguchi, T., Saika, A., Nomura, K., Watanabe, T., Watanabe, T., Fujimoto, Y., Enoki, M., Sato, T., Kato, C., Kanehiro,  
575 H., 2011. Biodegradation of aliphatic polyesters soaked in deep seawaters and isolation of poly( $\epsilon$ -caprolactone)-degrading  
576 bacteria. *Polymer Degradation and Stability* 96, 1397–1403. URL: <https://www.sciencedirect.com/science/article/pii/S014139101100108X>, doi:10.1016/j.polymdegradstab.2011.03.004.

577

578 Seonghun, K., Park, S., Lee, K., 2014. Fishing Performance of an Octopus minor Net Pot Made of Biodegradable Twines.  
579 *Turkish Journal of Fisheries and Aquatic Sciences* 14, 21–30. doi:10.4194/1303-2712-v14\_1\_03.

580

581 Seonghun, K., Pyungkwan, K., Seongjae, J., Kyoungsoon, L., 2020. Assessment of the physical characteristics and fishing  
582 performance of gillnets using biodegradable resin (PBS/PBAT and PBSAT) to reduce ghost fishing. *Aquatic Conservation: Marine and Freshwater Ecosystems* 30, 1868–1884. URL: <https://onlinelibrary.wiley.com/doi/abs/10.1002/aqc.3354>,  
583 doi:10.1002/aqc.3354.

584

585 Sisti, L., Totaro, G., Marchese, P., 2016. PBS Makes its Entrance into the Family of Biobased Plastics, in: *Biodegradable and Biobased Polymers for Environmental and Biomedical Applications*. John Wiley & Sons, Ltd, pp. 225–285. URL: <https://onlinelibrary.wiley.com/doi/abs/10.1002/9781119117360.ch7>.

586

587 Song, H., Lee, S.Y., 2006. Production of succinic acid by bacterial fermentation. *Enzyme and Microbial Technology* 39, 352–  
588 361. URL: <https://www.sciencedirect.com/science/article/pii/S0141022906001190>, doi:10.1016/j.enzmitec.2005.  
589 11.043.

590

591 Tachibana, Y., Kimura, S., Kasuya, K.i., 2015. Synthesis and Verification of Biobased Terephthalic Acid from Furfural. *Scientific Reports* 5, 8249. URL: <https://www.nature.com/articles/srep08249>, doi:10.1038/srep08249. number: 1 Publisher:  
592 Nature Publishing Group.

593

594 Thellen, C., Coyne, M., Froio, D., Auerbach, M., Wirsén, C., Ratto, J.A., 2008. A Processing, Characterization and Marine  
595 Biodegradation Study of Melt-Extruded Polyhydroxyalkanoate (PHA) Films. *Journal of Polymers and the Environment* 16,  
596 1–11. URL: <https://doi.org/10.1007/s10924-008-0079-6>, doi:10.1007/s10924-008-0079-6.

597

598 Tserki, V., Matzinos, P., Pavlidou, E., Vachliotis, D., Panayiotou, C., 2006. Biodegradable aliphatic polyesters. Part I.  
599 Properties and biodegradation of poly(butylene succinate-co-butylene adipate). *Polymer Degradation and Stability* 91, 367–  
376. URL: <https://www.sciencedirect.com/science/article/pii/S0141391005002089>, doi:10.1016/j.polymdegradstab.  
2005.04.035.

600

601 Van Cauwenberghe, L., Vanreusel, A., Mees, J., Janssen, C.R., 2013. Microplastic pollution in deep-sea sediments. *Environmental Pollution* 182, 495–499. URL: <https://www.sciencedirect.com/science/article/pii/S0269749113004387>,  
602 doi:10.1016/j.envpol.2013.08.013.

603

604 Volova, T.G., Boyandin, A.N., Vasiliev, A.D., Karpov, V.A., Prudnikova, S.V., Mishukova, O.V., Boyarskikh, U.A., Filipenko,  
605 M.L., Rudnev, V.P., Bá Xuân, B., Viêt Dũng, V., Gitelson, I.I., 2010. Biodegradation of polyhydroxyalkanoates (PHAs)  
606 in tropical coastal waters and identification of PHA-degrading bacteria. *Polymer Degradation and Stability* 95, 2350–2359.  
607 URL: <https://www.sciencedirect.com/science/article/pii/S0141391010003642>, doi:10.1016/j.polymdegradstab.2010.  
08.023.

- 608 Wang, Y.W., Mo, W., Yao, H., Wu, Q., Chen, J., Chen, G.Q., 2004. Biodegradation studies of poly(3-hydroxybutyrate-co-  
609 3-hydroxyhexanoate). *Polymer Degradation and Stability* 85, 815–821. URL: [https://www.sciencedirect.com/science/  
610 article/pii/S0141391004000825](https://www.sciencedirect.com/science/article/pii/S0141391004000825), doi:10.1016/j.polydegradstab.2004.02.010.
- 611 Wilcox, C., Hardesty, B.D., 2016. Biodegradable nets are not a panacea, but can contribute to addressing the ghost fishing  
612 problem. *Animal Conservation* 19, 322–323. URL: <https://onlinelibrary.wiley.com/doi/10.1111/acv.12300>, doi:10.  
613 1111/acv.12300.
- 614 Wright, L.S., Napper, I.E., Thompson, R.C., 2021. Potential microplastic release from beached fishing gear in Great Britain's  
615 region of highest fishing litter density. *Marine Pollution Bulletin* 173, 113115. URL: [https://www.sciencedirect.com/  
616 science/article/pii/S0025326X21011498](https://www.sciencedirect.com/science/article/pii/S0025326X21011498), doi:10.1016/j.marpolbul.2021.113115.
- 617 Wright, S.L., Thompson, R.C., Galloway, T.S., 2013. The physical impacts of microplastics on marine organisms: A review.  
618 *Environmental Pollution* 178, 483–492. URL: <https://www.sciencedirect.com/science/article/pii/S0269749113001140>,  
619 doi:10.1016/j.envpol.2013.02.031.
- 620 Xu, J., Guo, B.H., 2010. Poly(butylene succinate) and its copolymers: Research, development and industrialization. *Biotech-  
621 nology Journal* 5, 1149–1163. URL: <https://onlinelibrary.wiley.com/doi/abs/10.1002/biot.201000136>, doi:10.1002/  
622 biot.201000136.
- 623 Zettler, E.R., Mincer, T.J., Amaral-Zettler, L.A., 2013. Life in the “Plastisphere”: Microbial Communities on Plastic Marine  
624 Debris. *Environmental Science & Technology* 47, 7137–7146. URL: <https://doi.org/10.1021/es401288x>, doi:10.1021/  
625 es401288x. publisher: American Chemical Society.
- 626 Zhao, J.H., Wang, X.Q., Zeng, J., Yang, G., Shi, F.H., Yan, Q., 2005. Biodegradation of poly(butylene succinate) in compost.  
627 *Journal of Applied Polymer Science* 97, 2273–2278. URL: <https://onlinelibrary.wiley.com/doi/abs/10.1002/app.22009>,  
628 doi:10.1002/app.22009.
- 629 Zimmermann, L., Dombrowski, A., Völker, C., Wagner, M., 2020. Are bioplastics and plant-based materials safer than  
630 conventional plastics? In vitro toxicity and chemical composition. *Environment International* 145, 106066. URL: [https:  
631 //www.sciencedirect.com/science/article/pii/S0160412020320213](https://www.sciencedirect.com/science/article/pii/S0160412020320213), doi:10.1016/j.envint.2020.106066.